

# Engineering Specification for large-aperture UVO space telescopes derived from Science requirements

H. Philip Stahl<sup>a</sup>, Marc Postman<sup>b</sup>, and W. Scott Smith<sup>a</sup>

<sup>a</sup>NASA Marshall Space Flight Center; <sup>b</sup>Space Telescope Science Institute

## ABSTRACT

The Advance Mirror Technology Development (AMTD) project is a three year effort initiated in FY12 to mature by at least a half TRL step six critical technologies required to enable 4 to 8 meter UVOIR space telescope primary mirror assemblies for both general astrophysics and ultra-high contrast observations of exoplanets. AMTD uses a science-driven systems engineering approach. We mature technologies required to enable the highest priority science AND result in a high-performance low-cost low-risk system. To provide the science community with options, we are pursuing multiple technology paths. We have assembled an outstanding team from academia, industry, and government with extensive expertise in astrophysics and exoplanet characterization, and in the design/manufacture of monolithic and segmented space telescopes. A key accomplishment is deriving engineering specifications for advanced normal-incidence monolithic and segmented mirror systems needed to enable both general astrophysics and ultra-high contrast observations of exoplanets missions as a function of potential launch vehicles and their mass and volume constraints.

**Keywords:** Space Telescope Mirrors, Mirror Technology Development, Systems Engineering

## 1. INTRODUCTION

According to the NRC ASTRO2010 Decadal Survey<sup>1</sup>, an advanced large-aperture ultraviolet, optical, near-infrared (UVOIR) telescope is required to enable the next generation of compelling astrophysics and exoplanet science. Measurements at UVOIR wavelengths provide robust, often unique, diagnostics for studying a variety of astronomical environments and objects. UVOIR observations are responsible for much of our current astrophysics knowledge and will produce as-yet unimagined paradigm-shifting discoveries. A new, larger UVOIR telescope is needed to help answer fundamental scientific questions, such as: Does life on nearby Earth-like exoplanets? How do galaxies assemble their stellar populations? How do galaxies and the intergalactic medium interact? And, how did planets and smaller bodies in our own solar system form and evolve?

The Decadal also noted that present technology is not mature enough to affordably build and launch any potential UVOIR mission concept. And, per the NASA Office of Chief Technologist Science Instruments, Observatory and Sensor Systems Technology Assessment Roadmap<sup>2</sup>, technology to enable such a mission needs to be at a technology readiness level 6 (TRL6) by 2018 so that a viable flight mission can be proposed to the 2020 Decadal Review. Advanced Mirror Technology Development (AMTD) is a funded NASA Strategic Astrophysics Technology (SAT) project. Our objective is to systematically mature to TRL-6 the critical technologies needed to produce 4-m or larger flight-qualified UVOIR mirrors by 2018 so that a viable mission can be considered by the 2020 Decadal Review. These technologies must enable missions capable of both general astrophysics and ultra-high contrast exoplanet observations.

To enable the primary mirrors of potential future space telescopes, advances are required in 6 inter-linked technologies:

- *Large-Aperture, Low Areal Density, High Stiffness Mirrors:* 4 to 8 m monolithic and 8 to 16 m segmented primary mirrors require larger, thicker, stiffer substrates.
- *Support System:* Large-aperture mirrors require large support systems to ensure they survive launch and deploy on orbit in a stress-free and undistorted shape.
- *Mid/High Spatial Frequency Figure Error:* A very smooth mirror is critical for producing a high-quality point spread function (PSF) for high-contrast imaging.
- *Segment Edges:* Edges impact PSF for high-contrast imaging applications, contributes to stray light noise, and affects the total collecting aperture.
- *Segment-to-Segment Gap Phasing:* Segment phasing is critical for producing a high-quality temporally stable PSF.
- *Integrated Model Validation:* On-orbit performance determined by mechanical and thermal stability. Future systems require validated performance models.

Just as JWST's architecture was driven by launch vehicle, future mission architectures (regardless of whether they are monolithic, segmented or interferometric) will depend on the up-mass and volume capacities of future launch vehicles (and of course available budget). Since we cannot predict what the capacities of future launch vehicles will be, we must prepare for all potential futures. Therefore, to provide the science community with options, we are pursuing multiple technology paths. And, we are advancing all 6 technologies simultaneously, because all are required to make a primary mirror assembly (PMA) with the necessary on-orbit performance. On-orbit thermal and mechanical performance depends on PMA stiffness and the substrate's coefficient of thermal expansion (CTE) and thermal mass. PMA stiffness depends on substrate and support stiffness. The ability to cost-effectively eliminate mid/high spatial figure errors and polishing edges also depends on substrate stiffness. And, the ability to phase segments depends on structure stiffness.

AMTD uses a science-driven systems-engineering approach. We are maturing technologies required to enable both the highest priority science and a high-performance low-cost low-risk system. To accomplish our goals, we have assembled an outstanding team from academia, industry, and government with extensive expertise in astrophysics and exoplanet characterization; and in the design/manufacture of monolithic and segmented space telescopes. To insure that we mature the most relevant technology, we have derived engineering specifications for potential future monolithic and segmented space primary mirror systems needed to enable both general astrophysics and ultra-high contrast observations of exoplanets missions as a function of potential launch vehicle and its inherent mass and volume constraints.

## 2. TECHNICAL TEAM

AMTD uses a science-driven systems engineering approach which depends upon collaboration between a Science Advisory Team and a Systems Engineering Team. The two teams work collaboratively to insure that we mature technologies required to enable the highest priority science AND result in a high-performance low-cost low-risk system. The responsibilities of the Science and Engineering teams are to:

- derive engineering specifications for monolithic and segmented-aperture normal-incidence mirrors which flow down from the on-orbit performance needed to enable the required astrophysical measurements and flow up from implementation constraints,
- identify the technical challenges in meeting these engineering specifications,
- iterate between the science needs and engineering specification to mitigate the challenges, and
- prioritizing the technology development which yields the greatest on-orbit performance improvement for the lowest cost and risk.

To help predict on-orbit performance and assist in architecture trade studies, the Engineering team develops Structural, Thermal and Optical Performance (STOP) models of candidate mirror assembly systems including substrates, structures, and mechanisms. These models are validated by test of full- and subscale components in relevant thermo-vacuum environments. Specific analyses include: maximum mirror substrate size, first fundamental mode frequency (i.e., stiffness) and mass required to fabricate without quilting, survive launch, and achieve stable pointing and maximum thermal time constant.

The Science Advisory Team was assembled to provide AMTD with advice from experts in the area of UVOIR astrophysics, exoplanet characterization, and terrestrial and space telescope performance requirements. The Science team is chaired by Dr. Marc Postman of the Space Telescope Science Institute and consists of (in alphabetical order): Dr. Olivier Guyon, University of Arizona; John E. Krist, Jet Propulsion Laboratory; Dr. Bruce A. Macintosh, Lawrence Livermore National Laboratory; and Dr. Remi Soummer, Space Telescope Science Institute.

The Engineering Team was assembled based upon their expertise in the design, fabrication and testing of monolithic and segmented, large-aperture ground and UVOIR space telescopes. The Engineering team is chaired by Dr. H. Philip Stahl of NASA Marshall Space Flight Center and consists of engineers from NASA (in alphabetical order: Mr. William R. Arnold, NASA MSFC Contractor; Mr. Gary Mosier, NASA Goddard Space Flight Center; and Dr. W. Scott Smith); ITT Exelis and new team member Schott/Brashear.

### 3. SCIENCE REQUIREMENTS

UVOIR electromagnetic radiation is highly sensitive to many astrophysical processes. Measurements at these wavelengths provide robust, often unique, diagnostics for studying a variety of astronomical environments and objects. UVOIR observations are responsible for much of our current astrophysics knowledge and will produce as-yet unimagined paradigm-shifting discoveries. The National Research Council (NRC) Astro2010 Decadal Review recognized the importance of science enabled by a larger UV-optical space telescope to succeed the Hubble Space Telescope (HST). The science drivers for a few of the many exciting investigations requiring a next-generation large-aperture UVOIR space telescope are:

**“Are We Alone?”** Do Earth-sized planets exist in the Habitable Zones (HZ) of their host stars? Do any harbor life? The tools for answering the first question already exist (e.g., Kepler, CoRoT); those that can address the second require a large-aperture UVOIR telescope. Earth-mass planets are faint and detecting a biosignature like atmospheric oxygen requires direct spectroscopy. Such direct spectroscopy requires high-contrast imaging and starlight suppression factors of  $10^9$  to  $10^{10}$ . This is two orders of magnitude beyond what can be done with 30 to 40 m ground-based telescopes. Furthermore, planets with biosignatures may be rare, requiring a search of tens or even several hundred stars to find compelling signs of life. Given that the number of stars that can be surveyed scales approximately as  $D^3$  (where  $D$  is telescope diameter), an aperture size of at least 8 meters is required to maximize the chance for a successful search for life in the solar neighborhood.

**Reconstructing Assembly History of Galaxies.** To determine how and when galaxies assemble their stellar populations, scientists need knowledge of their star age distribution and how this assembly varies with environment. The most direct and accurate age diagnostic comes from resolving individual, older stars that comprise the main sequence turnoff. However, the main sequence turnoff rapidly becomes too faint to detect for any existing telescope observing galaxies beyond the Local Group. HST and JWST cannot reach any large galaxies besides our Milky Way and M31 because they lack the required angular resolution; therefore, a larger UVOIR space telescope is needed. An 8-meter space telescope can reach 10 gigayear (Gyr) old stars in 140 galaxies including 12 giant spirals and the nearest giant elliptical. A 16-meter space telescope extends our reach to the Coma Sculptor Cloud, netting a total of 370 galaxies including 45 giant spirals and 6 ellipticals. Such observations, in conjunction with those from large ground-based telescopes, will lead to a comprehensive and predictive theory of galaxy and star formation.

**Revealing Galaxy Halo and Gas Physics in Unprecedented Detail.** There is great scientific power in combining high spatial resolution with sensitive UV spectroscopy. One very important application is studying galaxy formation. We know that galaxies form and evolve, but little is known about how this happens. The physical processes involve complex interactions between baryonic matter in galaxies, energy exchanged during the birth and death of stars, gas outside galaxies in the intergalactic medium (IGM), other neighboring galaxies, and dark matter that dominates and shapes the underlying gravitational potential. Enabling deep and extensive spectroscopic probes of IGM, especially in the UV, provides the key data needed to solve this puzzle, particularly in the redshift range  $z < 3$  when the cosmic star formation rate peaks and then fades.

**Exploration of the Outer Solar System.** Exploration of our solar system is in a golden age. But there is still much to learn about how and why planets form and evolve. For example, long-term observations with a significantly more sensitive UV-optical telescope than HST would facilitate the search for endogenic activity on Europa; the chemical characterization of the tenuous atmosphere of Pluto; an expanded understanding of the influence of the solar wind on the outer solar system; and a better understanding of the influx of galactic cosmic rays on the origins of life.

To realize these ground-breaking scientific objectives, the AMTD Science Team, led by Dr. Postman, developed a set of science requirements to enable the most compelling science questions. Figure 1 shows a table which summarizes how science drivers map into telescope performance requirements for a UVOIR space telescope.

Table 2.1: Science Flow-down Requirements for a Large UVOIR Space Telescope			
Science Question	Science Requirements	Measurements Needed	Requirements
Is there life elsewhere in Galaxy?	Detect at least 10 Earth-like Planets in HZ with 95% confidence.	High contrast ( $\Delta\text{Mag} > 25$ mag) SNR=10 broadband ( $R = 5$ ) imaging with IWA $\sim 40$ mas for $\sim 100$ stars out to $\sim 20$ parsecs.	$\geq 8$ meter aperture Stable $10^{-10}$ starlight suppression
	Detect presence of habitability and bio-signatures in the spectra of Earth-like HZ planets	High contrast ( $\Delta\text{Mag} > 25$ mag) SNR=10 low-resolution ( $R=70-100$ ) spectroscopy with an IWA $\sim 40$ mas; spectral range 0.3 – 2.5 microns; Exposure times $< 500$ ksec	$\sim 0.1$ nm stable WFE per 2 hr $\sim 1.3$ to 1.6 mas pointing stability
What are star formation histories of galaxies?	Determine ages ( $\sim 1$ Gyr) and metallicities ( $\sim 0.2$ dex) of stellar populations over a broad range of galactic environments.	Color-magnitude diagrams of solar analog stars ( $V_{\text{mag}} \sim 35$ at 10 Mpc) in spiral, lenticular & elliptical galaxies using broadband imaging	$\geq 8$ meter aperture Symmetric PSF 500 nm diffraction limit
What are kinematic properties of Dark Matter	Determine mean mass density profile of high M/L dwarf Spheroidal Galaxies	0.1 mas resolution for proper motion of $\sim 200$ stars per galaxy accurate to $\sim 20 \mu\text{s}/\text{yr}$ at 50 kpc	1.3 to 1.6 mas pointing stability
How do galaxies & IGM interact and affect galaxy evolution?	Map properties & kinematics of intergalactic medium over contiguous sky regions at high spatial sampling to $\sim 10$ Mpc.	SNR = 20 high resolution UV spectroscopy ( $R = 20,000$ ) of quasars down to FUV mag = 24, survey wide areas in $< 2$ weeks	$\geq 4$ meter aperture
How do stars & planets interact with interstellar medium?	Measure UV Ly-alpha absorption due to Hydrogen “walls” from our heliosphere and astrospheres of nearby stars	High dynamic range, very high spectral resolution ( $R = 100,000$ ) UV spectroscopy with SNR = 100 for $V = 14$ mag stars	500 nm diffraction limit Sensitivity down to 100 nm wavelength.
How did outer solar system planets form & evolve?	UV spectroscopy of full disks of solar system bodies beyond 3 AU from Earth	SNR = 20 - 50 at spectral resolution of $R \sim 10,000$ in FUV for 20 AB mag	

Figure 1: Table 2.1 from the AMTD Proposal which summarizes the Science requirements for a future UVOIR space telescope.

## 4. ENGINEERING SPECIFICATIONS

The purpose of this effort is not to design a specific telescope for a specific mission or to work with a specific instrument. We are not producing an optical design or prescription. We are producing a set of primary mirror engineering specifications which will enable the on-orbit telescope performance required to enable the desired science. Our philosophy is to define a set of specifications which ‘envelop’ the most demanding requirements of all potential science. If the PMA meets these specifications, it should work with most potential science instrument. Defining mirror coating or contamination specifications is beyond the scope of the current effort. A future effort will define engineering specifications for the secondary mirror and support structure.

Both general astrophysics and exoplanet science contribute requirements, the most challenging requirements come from ultrahigh-contrast imaging to characterize exoplanets. The science requirements of proposed exoplanet and astrophysics missions were used to determine the sensitivity, signal to noise, diffraction limited performance, encircled energy, point spread function stability and thermal environment requirements. These requirements then determine the aperture and optical wavefront specifications for potential telescope assemblies which can fit inside current and planned launch vehicles. The optical wavefront specification becomes the top level of the error budget that is split into various sources that control the structural, thermal and optical design.

### 4.1 Aperture Size Specification

The most important specification is aperture size. And aperture size is driven by the need of exoplanet science to search enough star’s habitable zones and to characterize exoplanets in those habitable zones to identify at least 2 Earth twins.

To enable the **direct detection** of a terrestrial planet in the HZ, one needs to achieve an angular resolution that is roughly 0.50 times the size of the angular radius of the Habitable Zone. The habitable zone in our solar system extends from roughly 0.7 – 2 AU. The size of the HZ scales as  $(L^*/L_{\text{SUN}})^{0.5}$ . Table 1 gives the size of Habitable Zones for four different main sequence stellar classes<sup>3</sup>.

Main Sequence Spectral Class	Luminosity (Relative to Sun)	Habitable Zone Location (AU)	Angular radius of HZ at 10 pc (mas)	Telescope Diameter (meters)
M	0.001	0.022 – 0.063	2.2 – 6.3	90
K	0.1	0.22 – 0.63	22 – 63	8.9
G	1.0	0.7 – 2.0	70 – 200	2.7
F	8.0	1.98 – 5.66	198 – 566	1.0

The last column shows the telescope diameter that provides an angular resolution corresponding to 0.5 x HZ radius at 760 nm. The wavelength 760 nm is specified because it is a key biomarker (e.g., the 760 nm line of molecular oxygen). From TPF-C STDT report<sup>4</sup>:

*“For stars not too different from the Sun, planet detection is accomplished most easily at wavelengths in or just beyond the visible, 0.5-0.8  $\mu\text{m}$ , where the photon flux is highest and where silicon-based CCDs are most sensitive. Given sufficient spectral resolution ( $R \equiv \lambda/\Delta\lambda > 70$ ), this wavelength range would permit the detection of  $\text{O}_2$ ,  $\text{H}_2\text{O}$ , and possibly  $\text{O}_3$  on a planet like present Earth. Extended wavelength coverage to 1.1 microns, or even 1.7 microns, would be desirable. The strongest  $\text{O}_2$  band is the A band at 0.76  $\mu\text{m}$ .  $\text{O}_2$  is considered an excellent biomarker gas, at least for planets orbiting within the liquid water HZ.*

An additional criterion is that one must be able to obtain a SN=10 R=100 spectrum of the exoplanet in less than ~500 ksec. So collecting area coupled with resolution is the essential metric. Table 2 shows the number of F,G,K spectral class stars one can observe with a coronagraph on a space-based telescope as a function of telescope diameter.

Telescope Diameter (meters)	Number of F,G,K Stars Observed in a 5-year mission, yielding SNR=10 R=70 Spectrum of Earth-like Exoplanet
2	3
4	13
8	93
16	688

In 2012 Lyon and Clampin performed a similar analysis<sup>5</sup>. Figure 2 shows the number of stars (in the TPF-C database out to 30 parsecs) whose Habitable Zone (HZ) is larger than the inner working angle (IWA) of a telescope with a given diameter. For G class stars, an 8-meter aperture more than doubles the number of HZs which can be imaged, but a 16-m aperture only adds an additional 5 HZs. Where 16-m helps is for K and M class stars. The last column is the total time ( $\Delta t$ ) in days required to obtain a single SNR=5 R=5 (550 nm; FWHM 110) spectrum for each of the stars in the ‘Total’ column. Assuming that it takes 5 visits to completely search a system, multiplying the last column by 5 gives an estimate of the total mission length to characterize every HZ (i.e. assuming that  $\eta_{\text{EARTH}} = 1$ ). Observation time for different spectral resolution scales linearly. An R=50 spectra will take 10X longer than an R=5 spectra.

Table 1 Candidate stars versus aperture.

Diameter (meters)	IWA (mas)	Number of stars at or outside IWA						Total (575)	$\Delta t$ to SNR = 5
		A (18)	F (27)	G (124)	K (219)	M (163)	U (24)		
1 m	226.9	5	1	2	1	0	0	9	159.19
2 m	113.4	16	8	6	1	0	0	31	120.74
4 m	56.7	17	22	50	5	0	0	94	33.76
8 m	28.4	17	27	119	30	1	0	194	6.08
16 m	14.2	17	27	124	132	9	0	309	0.79

Figure 2: Table 1 from Lyon and Clampin showing number of stars whose Habitable Zones can be imaged.

Both of these analyses are for all available stars, but not every star may have an Earth twin. If the science requirement is to survey a sufficient number of stars,  $N_S$ , to find  $m$  earth like planets, then the telescope aperture must be sized to image approximately  $N_S = (m / \eta_{\text{EARTH}})$  stars. Table 3 provides some scenarios for the number of stars we will need to survey for different values of  $\eta_{\text{EARTH}}$  and for different telescope aperture sizes. Table 3 assumes a completeness of 100% on each target, which requires multiple visits to each star in case a planet (with any orbit radius) is at a projected separation inside the inner working angle of the optical system at one epoch. One can also survey double the number of stars with 50% statistical completeness to obtain the same number of detected planets.

Number of Earth-like Planets to Detect	$\eta_{\text{EARTH}}$	Number of Stars one needs to Survey	Minimum Telescope Diameter
2	0.03	67	8
2	0.15	13	4
2	0.30	7	4
5	0.03	167	10
5	0.15	33	8
5	0.30	17	6
10	0.03	333	16
10	0.15	67	8
10	0.30	33	8

An additional driver on the required aperture for a space telescope designed to characterize Earth-mass planets around a Sun-like star is the amount of exozodiacal light in the inner parts of the system. From TPF-C STDT report: “*TPF-C must be able to achieve [planet detection & characterization] under the assumption that all exoplanetary systems have an unknown quantity of exozodiacal dust of up to 3 zodis with an unknown pericenter shift of up to 0.07 AU.*”<sup>4</sup> This requirement places a constraint on the PSF; a sharper (higher resolution) PSF will provide increased contrast of a planet relative to a zodi disk. This favors a larger telescope, assuming the same coronagraph.

Based on our analysis, it is clear that a space telescope in the range of 4 meters to 8 meters is required to make the required observations. The results also argue for something closer to 8 meters to provide some headroom to allow progress even if  $\eta_{\text{EARTH}}$  is low. However, if  $\eta_{\text{EARTH}}$  is  $\ll 0.1$ , then telescopes with apertures of 10 meters or greater would be required. Given this analysis, the AMTD project will mature technologies for three telescope configurations: 4-meter monolithic, 8-meter monolithic, and 8-meter segmented.

#### 4.2 Telescope Wavefront and Primary Mirror Surface Specification

The general astrophysics science requirement for a diffraction limited performance telescope drives the total primary mirror (PM) surface specification and particularly the low-spatial frequency portion of that specification. The exoplanet science high-contrast imaging requirement drives the mid- and high-spatial frequency portion of the PM specification. Of particular importance to exoplanet science is temporal wavefront stability.

To have a telescope with 500 nm diffraction limited performance (Strehl ratio  $\sim 80\%$ ) requires a total system wavefront error (WFE) of approximately 38 nm rms. For a 4-m telescope, this results in a point spread function (PSF) of 32 milli-arc-seconds (mas). For an 8-m telescope, the PSF is 16 mas. Contributors to a total system WFE include the telescope, the science instruments and the spacecraft’s ability to maintain a stable telescope line of sight pointing (Figure 3). The telescope’s WFE consists of contributions from the primary mirror (PM), the secondary mirror (SM), the ability to attached the PM and SM to the structure and accurately align them to each other, and the ability of the structure to maintain that alignment on-orbit. Stability is the system level response of the telescope to both the thermal environment and mechanical disturbances.

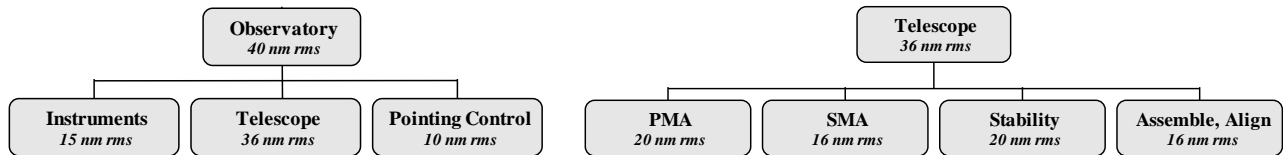


Figure 3: Simplified System Wavefront Error Budget Allocation Flowdown

Figure 4 shows how the PMA allocation of the total system WFE flows into the primary mirror engineering specifications. This is a nominal allocation and can be adjusted. The reader is reminded that surface error is half of wavefront error and that these specifications are independent of aperture size. The total PM surface figure specification can be further divided into low-, mid- and high-spatial frequency bands.

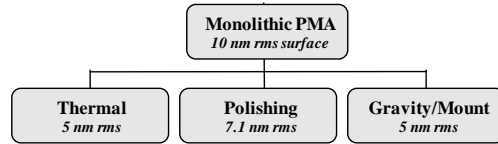


Figure 4: Primary Mirror Specification Allocation

As previously discussed, Exoplanet science wants to image planets in the Habitable Zone. But, for terrestrial mass planets in the HZ around G-type stars (e.g., the Sun), the ratio of reflected planet light to emitted starlight is  $\sim 10^{-10}$ . Thus, it is necessary to ‘block’ the light from the star in order to ‘see’ the planet. This is accomplished in a coronagraph. For a ‘perfect’ telescope, it is possible to create a mask to block the PSF produced by the star and pass the PSF of the planet. But, in a ‘real’ telescope, wavefront errors redistribute the light making it impossible to create the required  $10^{-10}$  contrast. As illustrated in figure 5a, low spatial frequency errors (typically called Figure errors) move energy from the core into the outer rings. Mid-spatial frequency errors blur or spread the core. And high-spatial frequency errors and surface roughness scatter light out of the core and over the entire PSF. Thus, while General Astrophysics science is most interested in the shape and stability of the PSF, Exoplanet science is particularly interested in mid- and high-spatial frequency errors move light from the host star out of the core and masks the light from the planet.

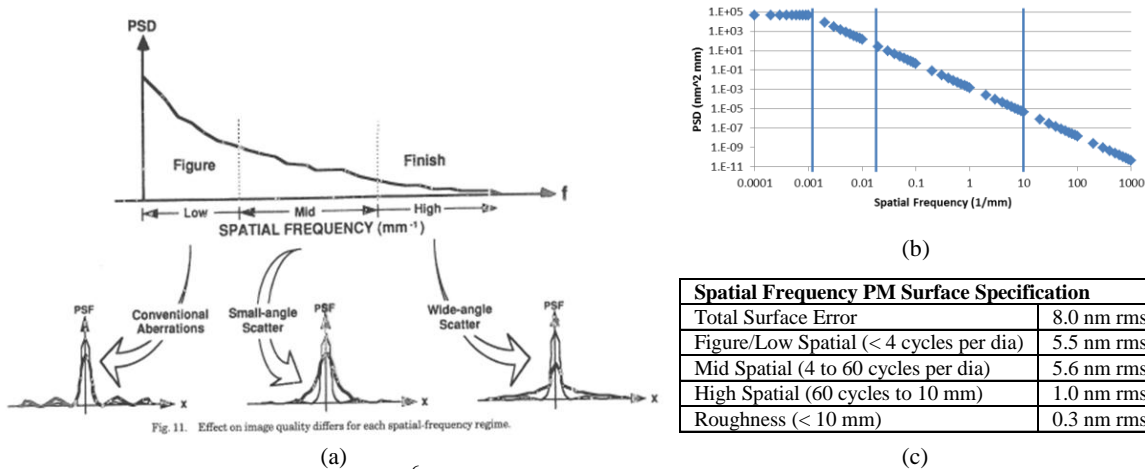


Figure 5: (a) Graphic from Harvey et. al.<sup>6</sup> showing effect on PSF of different spatial frequency bands; (b) enveloping PSD specification; (c) PSD spatial-band specification for an 8 nm rms surface based on a -2.25 PSD slope.

Typically, a surface is specified in terms of maximum RMS error for the total surface and for each spatial frequency band (Figure 5c) or Power Spectral Density (PSD) (Figure 5b). It is important to note that there is no accepted definition for the boundaries between different bands. They vary depending upon the science application need and manufacturing process. Surface errors can be controlled deterministically or stochastically. Polishing techniques exist using both large and small computer controlled laps to correct errors below a given spatial frequency (thus the ‘flat’ PSD). Above that spatial frequency, the surface error tends to be random, i.e. its PSD is a straight line with a negative slope. Systematic errors at higher spatial frequencies, such as quilting, manifest themselves as ‘peaks’ on this line.

Exoplanet science coronagraphs use deformable mirrors (DM) to create a ‘dark hole’ (Figure 6)<sup>7</sup> by correcting low-spatial frequency wavefront errors and moving light from the hole zone back into the core. A 64x64 DM can theoretically correct spatial frequencies up to 32 cycles per diameter (or half the number of DM elements). This could create a ‘dark hole’ with an inner working angle (IWA) of  $\lambda/D$  and an outer working angle (OWA) of  $32\lambda/D$ . But in practice, the limit is probably  $\sim 20$  cycles per diameter (or approximately a third the number of DM elements). The problem for exoplanet science is that primary mirror spatial frequency errors starting outside the

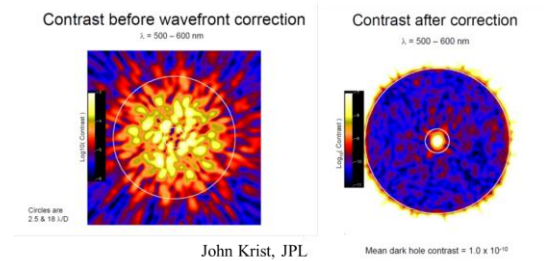


Figure 6: Exoplanet Dark Hole



OWA and extending up to 3X beyond what can be corrected by the DM can scatter energy back into the ‘dark hole’. Therefore, the primary mirror needs to be very smooth for these spatial frequency errors.

According to Shaklan<sup>8-9</sup>, the primary mirror should have < 4 nm rms for the spatial frequency band above 40 cycles per aperture diameter. And, a UVOIR mirror similar to Hubble (6.4 nm rms) or VLT (7.8 nm rms) can meet the requirements needed to provide a < 10-10 contrast ‘dark hole’ (Figure 7)<sup>9</sup>.

Please note: the surface error specification of < 10 nm rms applies equally to both monolithic and segmented aperture mirrors.

### 4.3 Telescope Wavefront Error Stability

Once a  $10^{-10}$  contrast dark hole has been created, the corrected wavefront phase must be stable to within a few picometers rms during science exposures to maintain the instantaneous (not averaged over integration time) speckle intensity to within  $10^{-11}$  contrast. Any temporal change in WFE can result in speckles which can produce a false exoplanet measurement or mask a true signal. WFE can vary with time due to the response of optics, structure and mounts to mechanical and thermal stimuli. Vibrations can be excited from reaction wheels, gyros, etc. And, thermal drift can occur from slew changes relative to Sun.<sup>7</sup>

Since it is impossible to make a telescope with zero instability, WFE must be actively controlled. It is our assumption that this active control is provided by DMs in the science instrument. And, we assume that the DMs can correct the WFE to the required ‘few’ picometers. Figure 8 illustrates a wavefront sense and control (WFSC) architecture that corrects the WFE of a telescope after a thermal slew to a few pico-meters and periodically updates that correction between observations.<sup>5</sup>

In this case, the stability of the telescope is determined by the observation time. For example, if the maximum desired science exposure is 2500 seconds (maximum exposure limited by cosmic ray hit rate), then the telescope WFE must be stable to < 25 pm rms for 2500 seconds. Alternatively, the WFSC system could operate parallel to the science observation. However, this correction process is still on the order of minutes.

Krist (Private Communication, 2013): wavefront changes to first 11 Zernikes can be measured with an accuracy of 5–8 pm rms in 60–120 sec on a 5<sup>th</sup> magnitude star in a 4 m telescope over a 500–600 nm pass band (using a reflection off occulter). Accuracy scales proportional to square root of exposure time or telescope area.

Lyon (Private Communication, 2013): 8 pm control takes ~64 sec for a Vega 0<sup>th</sup> mag star and 500–600 nm pass band [ $10^8$  photons/m<sup>2</sup>-sec-nm yield  $4.7 \times 10^5$  electrons/DOF and sensing error ~730  $\mu$ m = 64 pm at  $\lambda = 550$  nm]

Guyon (Private Communication, 2012): measuring a single sine wave to 0.8 pm amplitude on a Magnitude V=5 star with an 8-m diameter telescope and a 100 nm effective bandwidth takes 20 seconds. [Measurement needs  $10^{11}$  photons and V=5 star has  $10^6$  photons/m<sup>2</sup>-sec-nm.] But, controllability needs 3 to 10 measurements, thus stability period requirement is 3 to 10X the measurement period.

Ignoring that the period required to achieve a wavefront sensing measurement depends on the magnitude of the star and spectral pass band, a conservative specification for the primary mirror surface figure error stability might be:

- < 10 picometers rms per 800 seconds for a 4-meter primary mirror
- < 10 picometers rms per 200 seconds for an 8-meter primary mirror

If the primary mirror’s SFE changes (as a function of mechanical stimuli or thermal environment) more slowly than this specification, then the science instrument’s control system should be able to maintain the required  $10^{-11}$  contrast. Yet to be investigated is how this specification depends upon whether the temporal error is systematic, harmonic or random. Also, AMTD has not investigated the sensitivity of non-DM coronagraphs such as the visible nulling interferometer (VNC) to wavefront stability. But we believe that our specification is more demanding than the VNC’s need.

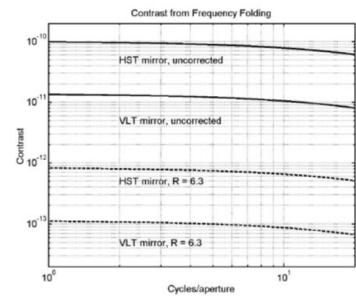


Figure 7. Contrast from frequency folding for spatial frequencies above 48 cycles per aperture, for an 8-m VLT primary and the 2.4 m HST primary. The uncompensated effect is above the required level of  $10^{-12}$  for both mirrors. The sequential DM configuration provides about ~100x reduction of the contrast when it compensates the center of a 100 nm bandpass centered at 633 nm. Both mirrors are acceptable after compensation. The frequency folding effect can be perfectly compensated by the Michelson configuration and is not present in the Visible Nuller.

Figure 7: From Shaklan & Green<sup>9</sup>, typical very smooth <10 nm rms mirrors can achieve  $10^{-10}$  contrast.

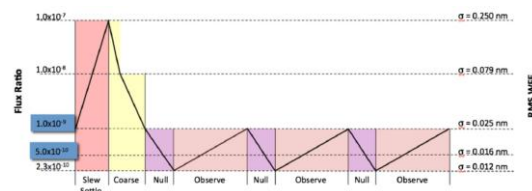


Figure 8: Illustration of active WFE control<sup>5</sup>



#### 4.4 Segmented Aperture

Regardless of whether the primary mirror is monolithic or segmented, to meet the astrophysics science requirements, it must have  $< 10$  nm rms surface. Segmenting the mirror increases complexity and redistributes the error allocations (Figure 9). The polishing allocation is for individual mirror segments. The phasing allocation is how well individual segments can be aligned. Please remember it is our assumption that any exoplanet instrument will have a segmented deformable mirror to further correct the primary mirror's surface figure error including segment to segment tip/tilt and co-phasing errors; and that any general astrophysics instrument will not have a DM.

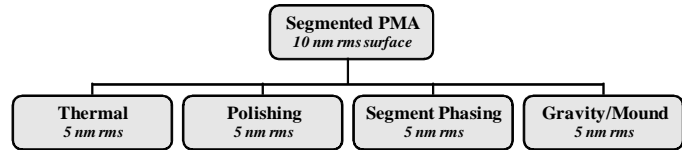


Figure 9: Notional segmented primary mirror surface error allocation

There are many different segmentation schemes, ranging from hexagonal segments to pie segments to multiple large circular mirrors. The selection and analysis of all potential segmentation patterns is beyond the scope of this effort. For this analysis we are assuming hexagonal segmentation and relying upon the published results of Yaitskova et al, 2003.<sup>10</sup> As shown in Figure 10, an aperture composed of hexagonal segments produces a complicated point spread function. The PSF for the telescope is found by taking the Fourier transform of the aperture function. The aperture function is described by a segment aperture convolved with a grid function. If one assumes that the segments are all identical (which in practice they are not) and that the grid function is regular (which in practice it is not), then the telescope PSF is described by the product of the PSF for the segments and the Grid( $\rho$ ) function (Fourier transform of the grid(r) function).

$$\text{PSF}_{\text{tel}} \sim \text{PSF}_{\text{seg}} \text{Grid}(\rho) \sim \mathcal{F}\{\text{segment} ** \text{grid}(r)\}$$

where:  $\text{PSF}_{\text{tel}} \text{ diameter} \sim \lambda/D_{\text{tel}}$        $\text{PSF}_{\text{seg}} \text{ diameter} \sim \lambda/d_{\text{seg}}$        $\text{Grid space} \sim \lambda/d_{\text{seg}}$

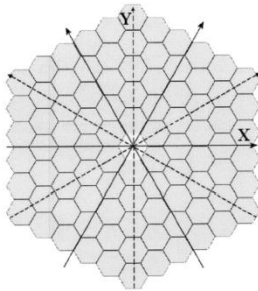


Fig. 1. Segmented mirror with segmentation order  $M = 5$  consisting of  $N = 90$  segments. Solid and dashed arrows illustrate the double  $\pi/3$  symmetry of the system.

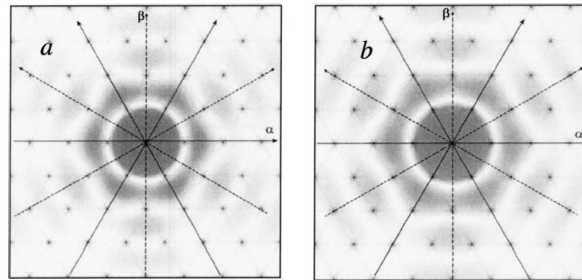


Fig. 2. a. Grid factor (regular spots) and the segment  $\text{PSF}_s$ , for a perfect telescope without gaps. Except for the central peak, all peaks of the grid factor fall into zeros of the segment  $\text{PSF}_s$ . Solid and dashed arrows illustrate the same double  $\pi/3$  symmetry as observed in the pupil plane (Fig. 1). b. The same, but with gaps between segments (relative gap size  $\omega=0.1$ ). Higher-order peaks are no longer coincident with  $\text{PSF}_s$  zeros. The same effect is seen for tip-tilt errors and segment-edge misfigure.

Figure 10: Figures 1 and 2 from Yaitskova et al, 2003 showing aperture segmentation, ideal PSF and PSF with gaps.

For a perfectly phased telescope with no gaps and optically perfect segments, the zeros of  $\text{PSF}_{\text{seg}}$  coincide with peaks of  $\text{Grid}(\rho)$  function resulting in a smooth  $\text{PSF}_{\text{tel}}$  with a central peak size  $\sim \lambda/D_{\text{tel}}$ . Unfortunately, real telescopes are not perfect. Gaps between segments, segment tip/tilt errors, rolled edges and surface figure errors change the shape or redistributes energy between rings of the  $\text{PSF}_{\text{seg}}$  without changing the  $\text{Grid}(\rho)$  function.<sup>10</sup> The effect is to produce a  $\text{PSF}_{\text{tel}}$  with energy at individual  $\text{Grid}(\rho)$  locations. This is illustrated in the right hand image of Figure 10. A segmented aperture with tip/tilt errors is like a blazed grating removing energy from the central core into higher-order peaks. If the error is 'static' then a segmented tip/tilt deformable mirror should be able to 'correct' the error. Any residual error should be 'fixed-pattern' and thus removable from the image. But, if error is 'dynamic' (e.g. the segments are rocking), then the higher-order peaks will 'wink'.

Segment to segment co-phasing or piston errors change the  $\text{Grid}(\rho)$  function but leave the  $\text{PSF}_{\text{seg}}$  unchanged, this results in a  $\text{PSF}_{\text{tel}}$  with speckles.<sup>10</sup> If the error is 'static' then a segmented piston deformable mirror should be able to 'correct' the error. Any residual error should be 'fixed-pattern' and thus removable from the image. But, if the error is 'dynamic', then speckles will move in the focal plane. Per Guyon<sup>11</sup>, the co-phasing specification required to achieve a given contrast level depends only on the total number of segments in the aperture and is independent of the telescope

diameter – the more segments; the more relaxed the co-phasing specification. And, the time required to control co-phasing depends only on telescope diameter (for a given magnitude star) and is independent of the number of segments – the larger the telescope diameter; the faster the control (Table 4). The reason for these two findings is: while it does take longer to measure a smaller segment’s co-phasing error because there are fewer photons, it takes less time to measure the larger co-phase error allowed by having more segments.

Table 4: Segment cophasing requirements for space-based telescopes  
(wavefront sensing done at  $\lambda=550\text{nm}$  with an effective spectral bandwidth  $\delta\lambda=100\text{ nm}$ )

Telescope diameter (D) & $\lambda$	Number of Segments (N)	Contrast	Target	Cophasing requirement	Stability timescale
4 m, 0.55 $\mu\text{m}$	10	1e-10	$m_v=8$	2.8 $\mu\text{m}$	22 mn
8 m, 0.55 $\mu\text{m}$	10	1e-10	$m_v=8$	2.8 $\mu\text{m}$	5.4 mn
8 m, 0.55 $\mu\text{m}$	100	1e-10	$m_v=8$	8.7 $\mu\text{m}$	5.4 mn

Regarding segment to segment gap distance, while an important contributor to PSF structure, from a practical perspective, it is by determined by architecture specific geometry and ‘non-interference’ issues and is beyond the scope of our study.

Regarding segment edge roll-off effects, because their error is static, their impact is limited.<sup>10, 12</sup> Also, the current state of the art does not appear to be overly limiting. JWST demonstrated 7 mm edges and SBIR contracts with QED and Zeeko have demonstrated 2 mm edges.<sup>13-14</sup>

One question which our study has not resolved is whether it is better to have fewer large segments or many small segments. If the goal is to produce a ‘dark hole’, then a highly segmented aperture (e.g. 32 segments per diameter in 16 rings) will have higher-order peaks that are beyond the outer working angle ( $16\lambda/D$ ). And, the more segments in the aperture, the larger the co-phasing specification. But, architectures with many small segments have the disadvantage of complexity; they require many mechanisms.

## 5. IMPLEMENTATION CONSTRAINTS

Developing a mission concept which meets the science requirements is only a half solution. The concept must also be able to survive launch and meet its on-orbit performance requirements. While one can conceive of mission concepts which might be launched on an EELV Heavy or an SLS or even a Falcon-9 Heavy, at present only the EELV Heavy actually exists<sup>15-16</sup>. For the purpose of this study, we will assume that any potential future space telescope mirror must be able to survive launch conditions similar to those produced by a Delta IV Heavy. All data in this section comes directly from the Delta IV Payload Planners Guide<sup>15</sup>. The launch loads, and vibro-acoustics will be discussed to provide a general idea of what the specifications of the mirror should be able to survive.

### 5.1 Launch Loads

During launch, payloads experience static and dynamic G loads. Static G-loads are produced by constant acceleration of the launch vehicle. Dynamic G-loads are produced by shocks such as when the payload is separated from the launch vehicle. Figure 11 shows the axial and lateral equivalent static G load combinations which, when applied to a spacecraft model (or mass and center of gravity location), envelop the spacecraft/launch vehicle interface loads. This diagram is typically called an airplane curve and is used for sizing and testing spacecraft primary bus structure. Figure 12 provides the minimum spacecraft mass and the spacecraft fundamental mode frequencies required to ensure that expected Coupled Loads Analysis (CLA) predicted spacecraft interface loads are likely to be bounded by application of the "airplane curve" load factors. This analysis can be used for determining preliminary structural testing needs for primary structural elements, but is not intended for deriving component (appendages like sensors, solar arrays, antennas) testing environments. Lighter spacecraft may have CLA spacecraft load factor predictions which are outside of the airplane curve. And spacecraft appendage elements will see even higher G loads. Verification of the preliminary load factors should be performed through CLA prior to testing.

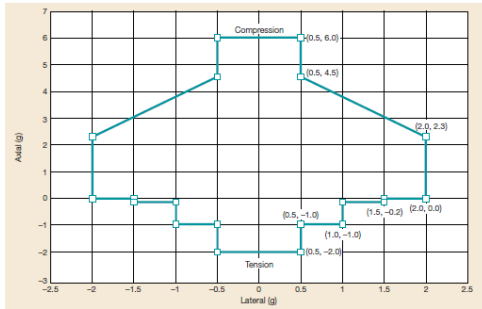


Figure 11: Design Load Factors for Delta IV Heavy

Static Envelope Requirements				
LV Type	Overall Payload Fairing length (M/ft)	Minimum Axial Frequency (Hz)	Minimum Lateral Frequency (Hz)	Minimum Weight (Kg/lb)
Delta IV Medium	11.7/38.5	27	8	907 (2000)
Delta IV M+(4,2)	11.7/38.5	27	8	2721 (6000)
Delta IV M+(5,2)	14.3/47	27	8	2721 (6000)
Delta IV M+(5,4)	14.3/47	27	8	4989 (11,000)
Delta IV Heavy	19.8/62.7	30	8	6577 (14,500)

Figure 11: Delta IV-H Quasi-Static Load Conditions

### 5.1 Vibro-Acoustic Environment

During launch, payloads experience loads from the mechanical transmission of vibration from the on-board rocket engines, as well as from the primary bus engines. They also experience loads from acoustic fields generated by the engines. The acceleration spectral density (ASD) determines the maximum predicted vibration environment. The maximum acoustic environment is the fluctuation of pressure on all surfaces of the launch vehicle and spacecraft. The maximum expected acoustic conditions occur during liftoff and powered flight. The acoustic environment is identified as the sound pressure level (SPL) and measured on a one-third octave band over a frequency range of 31.5 to 10,000 Hz, Figure 13. The acoustic test tolerances are +4/-2 db from 50 Hz to 2000 Hz. Any frequencies that fall above these acoustic test levels should be maintained relative to the nominal test levels. From Figure 13, the overall sound pressure level should be maintained within a tolerance of +3/-1 db.

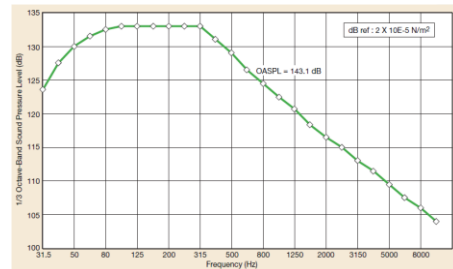


Figure 13: Delta IV-H 5m Composite Fairing Internal Acoustics Prediction

## 6. TECHNOLOGY CHALLENGES

Once one has fully defined the science requirements and the implementation constraints, it is possible to determine the technical challenges which must be overcome to enable any given ‘representative’ mission architecture. Figure 14 shows how science requirements (from Figure 1) flow into technical challenges for four different potential UVOIR missions. The engineering requirements for these four ‘representative’ missions are differentiated by implementation constraints of potential launch vehicle fairing diameter and mass capacity. These ‘representative’ mission architectures are: a 4-m monolith launched on an EELV, an 8-m monolith on a HLLV, an 8-m segmented on an EELV, or a 16-m segmented on a HLLV. Additionally, a Falcon 9-Heavy might enable a 4-m monolithic or an 8-m segmented telescope.

For all potential mission architectures, mass is the most important factor in the ability of a mirror to survive launch and meet its required on-orbit performance. More massive mirrors are stiffer and thus easier and less expensive to fabricate. More massive mirrors also are more mechanically and thermally stable. However, mass is highly constrained on launch vehicles<sup>16</sup>. Regardless of the telescope aperture, any mission to be launched on an EELV will have a primary mirror mass of approx. 740 kg (HST’s mirror is 740 kg and JWST’s mirror is 720 kg). Dividing by the desired collecting area yields the maximum required areal density. A HLLV could launch telescopes with a mirror mass of up to 25 mt. And, a Falcon-9 Heavy could launch a 4-m monolithic or 8-m segmented mirror of approximately 1500 kg mass.

Table 3.1: Science Requirement to Technology Need Flow Down				
Science	Mission	Constraint	Capability	Technology Challenge
Sensitivity	Aperture	EELV 5 m Fairing, 6.5 mt to SEL2	4 m Monolith	4 m, 200 Hz, 60 kg/m <sup>2</sup>
			8 m Segmented	4 m support system
		HLLV-Medium 10 m Fairing, 40 mt to SEL2	8 m Monolith	2 m, 200 Hz, 15 kg/m <sup>2</sup>
			16 m Segmented	8 m deployed support
		HLLV-Heavy 10 m Fairing, 60 mt to SEL2	8 m Monolith	8 m, <100Hz, 200kg/m <sup>2</sup>
			16 m Segmented	8 m, 10 mt support
	2 hr Exposure	Thermal 280K ± 0.5K 0.1K per 10min	< 5 nm rms per K	2-4m, 200Hz, 50kg/m <sup>2</sup>
			> 20 hr thermal time constant	16 m deployed support
		Dynamics TBD micro-g	< 5 nm rms figure	8m, <100Hz, 480kg/m <sup>2</sup>
				8 m, 20 mt support
Reflectance	Substrate Size	> 98% 100-2500 nm	2-4m, 200Hz, 120kg/m <sup>2</sup>	
			16 m deployed support	
High Contrast	Diffraction Limit	Monolithic	< 10 nm rms figure	low CTE material
			< 5 nm rms figure	thermal mass
		Segmented	< 2 mm edges	passive isolation
			< 1 nm rms phasing	active isolation
				Beyond Scope

Figure 14: Table 3.1 from the AMTD Proposal which summarizes the flow down of Science requirements to Technology needs.

## 7. CONCLUSIONS

The Advance Mirror Technology Development (AMTD) project is a three year effort initiated in FY12 to mature by at least a half TRL step six critical technologies required to enable 4 to 8 meter UVOIR space telescope primary mirror assemblies for both general astrophysics and ultra-high contrast observations of exoplanets.

- *Large-Aperture, Low Areal Density, High Stiffness Mirror Substrates*
- *Support System*
- *Mid/High Spatial Frequency Figure Error*
- *Segment Edges*
- *Segment to Segment Gap Phasing*
- *Integrated Model Validation*

Our objective is to mature to TRL-6 the critical technologies needed to produce 4-m or larger flight-qualified UVOIR mirrors by 2018 so that a viable mission can be considered by the 2020 Decadal Review. To provide the science community with options, we are pursuing multiple technology paths including both monolithic and segmented space mirrors. Thus far, AMTD has achieved all of its goals and accomplished all of its milestones.

AMTD uses a science-driven systems engineering approach. We mature technologies required to enable the highest priority science AND result in a high-performance low-cost low-risk system. To determine the highest priority technologies to mature, the AMTD Science Team and Engineering Team derived engineering specifications for advanced normal-incidence mirror systems needed to make the required science measurements.

## ACKNOWLEDGEMENTS

The authors wish to acknowledge very helpful conversations and technical reviews from John Krist, Oliver Guyon, Rick Lyon, and Stuart Shaklan. Work is funded by NASA Strategic Astrophysics Technology grant NASA 10-SAT10-0048.

## BIBLIOGRAPHY

1. *New Worlds, New Horizons in Astronomy and Astrophysics*, NRC Decadal Survey, 2010.
2. *Science Instruments, Observatories and Sensor Systems*, Technology Area 8 Roadmap, Office of the Chief Technologist, October 2010.
3. Mountain, M., van der Marel, R., Soummer, R., et al. 2009, astro2010: The Astronomy and Astrophysics Decadal Survey, 2010
4. TPF-C STDT Report: [http://exep.jpl.nasa.gov/files/exep/STDT\\_Report\\_Final\\_Ex2FF86A.pdf](http://exep.jpl.nasa.gov/files/exep/STDT_Report_Final_Ex2FF86A.pdf)
5. Lyon, Richard and Mark Clampin, "Space telescope sensitivity and controls for exoplanet imaging", *Optical Engineering*, Volume 51, No 1, January 2012
6. Harvey, Lewotsky and Kotha, "Effects of surface scatter on the optical performance of x-ray synchrotron beam-line mirrors", *Applied Optics*, Vol. 34, No. 16, pp.3024, 1995.
7. Krist, Trauger, Unwin and Traub, "End-to-end coronagraphic modeling including a low-order wavefront sensor", *SPIE Vol. 8422*, 844253, 2012; doi: 10.1117/12.927143
8. Shaklan, Green and Palacios, "TPFC Optical Surface Requirements", *SPIE 626511-12*, 2006.
9. Shaklan & Green, "Reflectivity and optical surface height requirements in a coronagraph", *Applied Optics*, 2006
10. Yaitskova, Dohlen and Dierickx, "Analytical study of diffraction effects in extremely large segmented telescopes", *JOSA*, Vol.20, No.8, Aug 2003.
11. Guyon, "Coronagraphic performance with segmented apertures: effect of cophasing errors and stability requirements", Private Communication, 2012.
12. Yaitskova and Troy, "Rolled edges and phasing of segmented telescopes", *Applied Optics*, Vol.50, No.4, 1 Feb 2011.
13. QED - NASA SBIR 03-S2.05-7100.
14. Zeeko - NASA SBIR 04-S2.04-9574.
15. Delta IV Payload Planners Guide, United Launch Alliance, Sept 2007
16. Stahl, H. Philip, Phil Sumrall, and Randall Hopkins, "Ares V launch vehicle: an enabling capability for future space science missions", *Acta Astronautica*, Elsevier Ltd., 2009, doi:10.1016/j.actaastro.2008.12.017